Revista Mexicana de Astronomía y Astrofísica, **35**, 173–185 (1999)

OPTICAL SPECTROSCOPY OF THE CENTRAL REGIONS OF BRIGHT BARRED SPIRAL GALAXIES

J. A. García-Barreto,[1] H. Aceves,[2] O. Kuhn,[3] G. Canalizo,[4]
R. Carrillo,[1] and J. Franco[1]

Received 1998 August 11; accepted 1999 September 3

RESUMEN

Se presentan espectros ópticos en la banda roja de 18 galaxias espirales con barra. El estudio se enfoca a la determinación de la cinemática local y condiciones del gas ionizado en el núcleo compacto (dentro de un diámetro de 5″), y en las regiones circunnucleares (dentro de un diámetro de 20″). Sólo 8 galaxias presentan emisión brillante al este y oeste del núcleo compacto. En otras 10, las líneas de emisión son débiles y sólo pudimos obtener un espectro promedio de la emisión central. No se detectaron líneas de emisión en las otras 8 galaxias. Se presenta una estimación de la masa dinámica en la región central de cada galaxia, en base a las velocidades observadas en las regiones circunnucleares. En NGC 4314 y NGC 6951, que presentan emisión de Hα distribuida en estructura de anillo alrededor del núcleo compacto, se determinan los cocientes [N II] λ6583/Hα y [S II]/Hα para ambos lados del anillo. La diferencia de velocidades en uno y otro lado, se usa como indicativo de la velocidad de rotación del gas alrededor del núcleo de la galaxia. Las velocidades encontradas en las las regiones circunnucleares en NGC 4314 y NGC 6951 explican naturalmente la discrepancia que existe en la literatura sobre las velocidades de recesión reportadas. Se encuentra que los cocientes [N II] λ6583/Hα y [S II]/Hα son diferentes en cada lado del anillo (un factor de $\sim$ 2 mayor en el lado oeste) y se infiere que las condiciones físicas son diferentes. El cociente [N II] λ6583/Hα en el núcleo de NGC 6951 es un factor de 2 mayor, comparado con el valor de la región oeste. Las densidades electrónicas se han estimado de los cocientes de líneas de azufre [S II].

ABSTRACT

Optical red spectra of a set of 18 bright barred spiral galaxies are presented. The study is aimed at determining the local kinematics and physical conditions of ionized gas in the compact nucleus (inside a diameter of 5″) and in the circumnuclear regions (inside a diameter of 20″). Only 8 galaxies showed bright emission from their east and west side of the nucleus. The spectrum of each region was analized separately. In other 10 galaxies the line emission was so weak that we were only able to obtain an average spectrum of the central emission. No emission was detected in the remaining 8 galaxies. An estimate of the dynamical mass is presented, based on the observed velocities in the circumnuclear regions. In NGC 4314 and NGC 6951, that show Hα emission distributed in circumnuclear ring structures, we determine the [N II] λ6583/Hα and [S II]/Hα ratios for the eastern and western regions of the rings. The velocity difference for the two sides is used to derive the rotation of the gas around the compact nucleus. The ratio, [N II] λ6583/Hα, is a factor of 2 larger in the compact nucleus of NGC 6951 than in its western side. The electron gas densities have been estimated from the [S II] lines ratio.

Key words: **GALAXIES: INDIVIDUAL: NGC 3504, NGC 4314, NGC 4691, NGC 5135, NGC 5383, NGC 5534, NGC 5915, NGC 6951 — GALAXIES: KINEMATICS AND DYNAMICS — GALAXIES: SPIRAL**

[1] Instituto de Astronomía, Universidad Nacional Autónoma de México.
[2] Instituto de Astrofísica de Andalucía, Spain.
[3] Observatorio Astronómico Nacional, UNAM, México.
[4] Institute for Astronomy, University of Hawaii, U.S.A.

1. INTRODUCTION

The study of emission lines in spiral galaxies has proven to be very useful in determining the distribution of ionized gas, and the physical conditions at the central regions (Burbidge & Burbidge 1960a,b, 1962, 1964, 1965; Burbidge, Burbidge, & Pendergast 1960; Keel 1983a,b; Kennicutt & Kent 1983; Heckman, Balick, & Crane 1980; Stauffer 1982a,b; Kennicutt 1992a,b; Appenzeller & Östreicher 1988; Filippenko & Sargent 1985; Ho, Filippenko, & Sargent 1995, 1997a,b; Vaceli et al. 1997).

Optical observations of barred spiral galaxies usually show the presence of symmetric structures around their center (presumably in the plane of the disk) which are referred to as *rings* (e.g., Buta 1986, 1995; Buta & Croker 1991). These symmetric structures are observed at different radii in their host galaxy; some are seen as extended structures at $\approx 10 - 15$ kpc from the center, but some others are located at about $4 - 5$ kpc, and there are circumnuclear rings at $300 - 900$ pc from the compact nucleus (e.g., Arsenault et al. 1988; Pogge 1989a,b; García-Barreto et al. 1991a,b, 1996; Barth et al. 1995; Genzel et al. 1995). A dynamical explanation for the origin of the structures, has been sought in terms of non-symmetric perturbations to the 'normal' gravitational potential of spiral galaxies (Binney & Tremaine 1987). The standard model to explain the formation of circumnuclear structures requieres knowledge of the angular velocity of the gas and stars (Ω_g), the epicyclic frequencies (κ), and an estimate of the angular velocity of the bar (Ω_b). In this model, it is generally assumed that the gravitational potential of the bar and Ω_b are independent of time (Binney & Tremaine 1987). Some of these galaxies have nearby neighbors and many numerical models have been carried out to examine the possible role of tidal interactions in the formation of bars and symmetric structures (e.g., Noguchi 1988; Friedli & Benz 1993).

Previous spectra of Shapley Ames Galaxies (Filippenko & Sargent 1985; Ho et al. 1995, 1997a,b) represent the emission of the innermost $2'' \times 7''$ or $r \leq 200$ pc. We present here new optical spectroscopic observations of the central regions of 18 barred galaxies using a long slit. Our main purpose is to provide local velocities and line ratios from the emission lines of [N II], Hα, and [S II], for both the nucleus and the circumnuclear regions. We have tried to obtain spectra of the compact nucleus and from the immediate surroundings separately (in the east and west directions since the slit was oriented at PA $\sim 90°$ E of N) by adding only the corresponding pixels in the slit. A clear example of this is in NGC 6951, where the spatial distribution of Hα shows the compact nucleus in addition to a circumnuclear ring. NGC 4314 also presents the circumnuclear ring in Hα, but no emission from the compact nucleus is detected in this case. In other six galaxies, the spatial distribution of the Hα emission is more diffuse. In 10 galaxies we were only able to obtain a spectrum of the central emission: compact nucleus and weak (if present at all) extranuclear emission.

The present work is divided as follows. In § 2, the selection criteria for the set of galaxies observed are established, and the observations are described. In § 3, our results are presented and discussed. In § 4, a brief summary is presented.

2. SAMPLE AND OBSERVATIONS

The galaxies studied here are part of an ongoing study of barred galaxies (see García-Barreto et al. 1993, 1996) and they were chosen using the following criteria: 1) bright barred galaxies in the Shapley Ames Catalog (first or second edition Sandage & Tammann 1987), 2) with declinations within a range accessible from San Pedro Mártir, $-41° \leq \delta \leq +70°$, and 3) with *IRAS* colors characteristic of star-forming galaxies according to Helou (1986; with $\log(f(12)/f(25)) \leq -0.15$ and $\log(f(60)/f(100)) \leq -0.1$) or equivalently, an *IRAS* dust temperature $T_d \geq 25$ K. The characteristics of each galaxy such as distance, *IRAS* fluxes, radio continuum fluxes, dust temperature, blue luminosity, H I mass, X-ray luminosity and inclination, are summarized in García-Barreto et al. (1993; 1996). The purpose of the observations was to determine the physical conditions (velocities and line ratios) from the innermost central regions (circumnuclear structure and compact nucleus). The slit length and width were selected accordingly. Table 1 lists the systemic velocities from optical, H I and CO observations taken from the literature, as well as whether a given galaxy shows Hα emission from either the compact nuclear region (innermost $5''$ in diameter) and/or circumnuclear regions (innermost $20''$ in diameter) (i.e., Pogge 1989a,b; García-Barreto et al. 1996).

The optical observations were performed at the Observatorio Astronómico Nacional at San Pedro Mártir, Baja California, México, on 1993, May 28, 29, 30, 31, and June 1, using the 2.12-m telescope f/7.5 equipped with a 1024×1024 Thompson CCD detector coupled to a Boller & Chivens spectrograph with 600 grooves per mm at a grating angle of 13°. The central wavelength was chosen in the red part of the spectrum, in order to include the [N II], Hα, and [S II] lines. The detector scale gives a 1.6 Å pixel^{-1} spectral resolution and a spatial resolution of $0''.73$ pixel^{-1} in the spectroscopic mode. The average seeing was about $1''.7$. The original slit length was 80 pixels long (or $58''$). The width of the slit was ~ 200 μm that translates to $\sim 2''.3$ on the sky, positioned at PA $\sim 90°$ (E of N), that is, east-west. In order to avoid edge effects at the moment of spectral calibration, we discarded in the final analysis altogether the outermost 21 pixels from the slit length (11 from one side and 10 from the other), and thus

TABLE 1

OBSERVED GALAXIES

Galaxy[a]	Optical[b]	HI[c]	CO[d]	i^e	PA^e_{bar}	CiNE[f]	CoNE[f]
3504	1535 ± 19	1538	1550	35	145	N	Y
4123	1325 ± 10	1327	...	39	105	N	Y
4314	883 ± 85	982	985	30	145	Y	N
4477	1263 ± 75	1263	...	26	15	?	?
4691	1123 ± 13	1119	1124	32	85	Y?	Y?
5135	4157 ± 35	4157	...	67	125	Y	Y
5347	2373 ± 12	2386	...	37	100	Y	Y
5383	2260 ± 3	2264	...	40	130	Y?	Y
5430	2875 ± 90	2960	2981	...	145	N	Y
5534	2633 ± 10	2633	...	...	80	N	Y
5597	2624 ± 66	...	...	...	55	Y	Y
5691	1876 ± 50	...	...	34	90	Y?	Y
5728	2970 ± 40	2780	...	65	35	Y	Y?
5757	2771 ± 58	...	...	32	165	Y	N
5915	2273 ± 14	2274	...	42	90	Y?	Y?
6239	938 ± 12	931	...	67	115	N	Y?
6907	3155 ± 80	3139	...	...	45	Y	Y
6951	1425 ± 10	1426	1464	28	85	Y	Y

[a] NGC catalog numbers.

[b] Systemic velocity in km s^{-1} from the Revised Shapley Ames Catalog (Sandage & Tammann 1987)

[c] Systemic velocity in km s^{-1} from Huchtmeier & Richter (1989), except for NGC 4314, in which we used the value observed by García-Barreto, Downes, & Huchtmeier (1994).

[d] Systemic velocity in km s^{-1} from Young et al. (1995) for most of the galaxies, except for NGC 4314 taken from García-Barreto et al. (1991b).

[e] Inclination of the galaxy's disk with respect to the plane of the sky; position angle of the stellar bar measured east of north taken from Tully (1988) or Huchtmeier & Richter (1989).

[f] Observed spatial Hα+[N II] emission: circumnuclear or extranuclear (innermost 20″) (CiNE); compact nucleus (innermost 5″) (CoNE) from Pogge (1989a,b), García-Barreto et al. (1996).

the final slit length was only 59 pixels or 43″. Only emission from about 19″ on each side of a central region of a galaxy was observed assuming that the compact nucleus was positioned in the middle of the slit covering the innermost 7 pixels.

The slit was positioned on the brightest optical region of each galaxy, at the declination corresponding to the compact nucleus. Figure 1 shows a sketch of the relative position of the slit with respect to a circumnuclear structure in the innermost central region of a galaxy. The position of the slit, however, did not coincide either with the position angle of the stellar bar and neither with the position angle of the line of nodes. Final velocity analysis showed that in some galaxies, the slit was off nucleus by a few arcseconds.

The on source time was 1200s for all the galaxies in the list (except for NGC 5915 which was observed for only 900s). Each galaxy observation was followed by a 1 second exposure of a tungsten lamp. Spectrophotometric standard stars PG1545+035, PG1708+602, and HD 192281 (Massey et al. 1988) and LTT6248 (Hamuy et al. 1992), were observed each night to calibrate in flux; integration time on HD 192281 and PG1545 was 60s, on LTT6248 it was 300s, and on PG1708 it was 480s. Dome flats taken every night with the same instrumental setup were used to flatten each galaxy spectrum. The data were bias-subtracted and flat-fielded using the NOAO IRAF software. The sky was subtracted with the IRAF task background using for each galaxy the apertures without any line emission (usually on the edges of the slit).

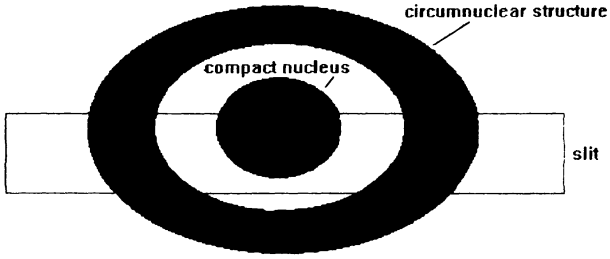

Fig. 1. Sketch (not to scale) of the slit position relative to a circumnuclear region in the central region of a given galaxy. The slit in all cases was positioned at PA 90° or east-west. Final length of slit was 59 pixels long or 43″, and 200 μm wide or 2.″3.

Not all the galaxies had emission away from the central pixels which correspond to the nucleus. Our original list of galaxies was 26, but we only detected emission lines in the spectra of 18 of them. Eight out of 18 showed emission from the east and west side of the central regions, and 6 out of 8 showed emission from their compact nuclear region as well. In the end, we extracted three different final spectra from each of the eight galaxies. In order to extract the final spectra we used the IRAF task "apall" where we co-added the pixels that correspond to each region. The numbers of pixels that were co-added to create each spectrum are given in the third column of Table 2. In none of the galaxies did we detect emission from the complete disk, and thus, no rotation curve could

TABLE 2

EMISSION LINES OF GALAXIES WITH CIRCUMNUCLEAR REGIONS

Gal.	Reg.	Pix[a]	[N II][b]	[N II]/Hα	Hα[b]	FWHM[c]	Hα Flux[d]	[N II][b]	[N II]/Hα	[S II][b]	[S II]/Hα	[S II][b]	[S II]/Hα
3504	E	6	1385	0.17	1383	215	12.0	1391	0.53	1403	0.13	1413	0.12
	W	3	1475	0.17	1470	237	9.7	1476	0.57	1498	0.13	1489	0.13
	N	6	1430	0.17	1422	253	11.0	1434	0.60	1440	0.12	1445	0.13
4314	E	12	935	0.13	868	237	1.6	853	0.45	903	0.09	913	0.18
	W	11	997	0.21	983	224	1.0	945	0.85	891	0.18	938	0.25
4691	E	9	1017	$\leq$ 0.01	1050	151	2.4	1062	0.38	1025	0.08	1066	0.07
	W	6	1038	0.07	1055	210	4.8	1059	0.41	1039	0.10	1073	0.09
	W[e]	11	...	...	635	1475	38.9	...	...	...	...	...	...
	N	6	1068	0.11	1068	207	16.4	1081	0.42	1091	0.09	1089	0.09
5135	E	5	3996	0.15	3965	279	1.1	3961	0.77	3783	0.21	3954	0.16
	W	4	4021	0.29	3988	247	7.1	3896	0.89	3995	0.17	4024	0.19
	N	4	3970	0.25	3966	334	19.9	3954	0.76	3962	0.15	3991	0.13
5383	E	14	2589	0.10	2453	224	2.3	2403	0.13	2433	0.14	2829	0.10
	W	13	2240	0.06	2257	219	5.4	2265	0.25	2271	0.10	2202	0.08
5534	E	13	2487	0.14	2477	233	11.1	2483	0.45	2497	0.15	2504	0.14
	W	14	2440	0.05	2502	173	0.9	2510	0.27	2531	0.11	2651	0.14
5915	E	18	2192	0.09	2207	196	1.5	2216	0.26	2151	0.07	2348	0.09
	W	12	2094	0.16	2061	201	1.6	2091	0.41	2061	0.18	2097	0.14
	N	8	2148	0.18	2133	259	2.9	2147	0.49	2127	0.21	2185	0.14
6951	E	6	1517	0.15	1491	247	1.1	1485	0.48	1652	0.09	1607	0.10
	W	4	1399	0.28	1348	251	1.1	1371	0.93	1215	0.08	1228	0.09
	N	7	1389	0.85	1428	285	0.8	1397	1.99	1423	0.32	1398	0.36

[a] Pixels added in slit for each region to produce the final spectra.

[b] Observed heliocentric velocity centroids in km s^{-1}. The velocity centroid uncertainties amount to about 25 km s^{-1} as a result of wavelength calibration and gaussian fitting. Columns 4 and 5 correspond to [N II] λ6548.1 Å; columns 9 and 10 to [N II] λ6583.4 Å; columns 11 and 12 to [S II] λ6716.4 Å, and columns 13 and 14 to [S II] λ6730.8 Å.

[c] Hα full width at half maximum, in km s^{-1}, after deconvolution with an instrumental response (FWHM$_{inst}\sim$ 3.23 $\pm$ 0.1 Å = 145 $\pm$ 5 km s^{-1}).

[d] Hα flux in units of 10^{-14} ergs s^{-1} cm^{-2}.

[e] Broadline from a western spectrum 12″, away from the spectrum of narrow lines (García-Barreto et al. 1995).

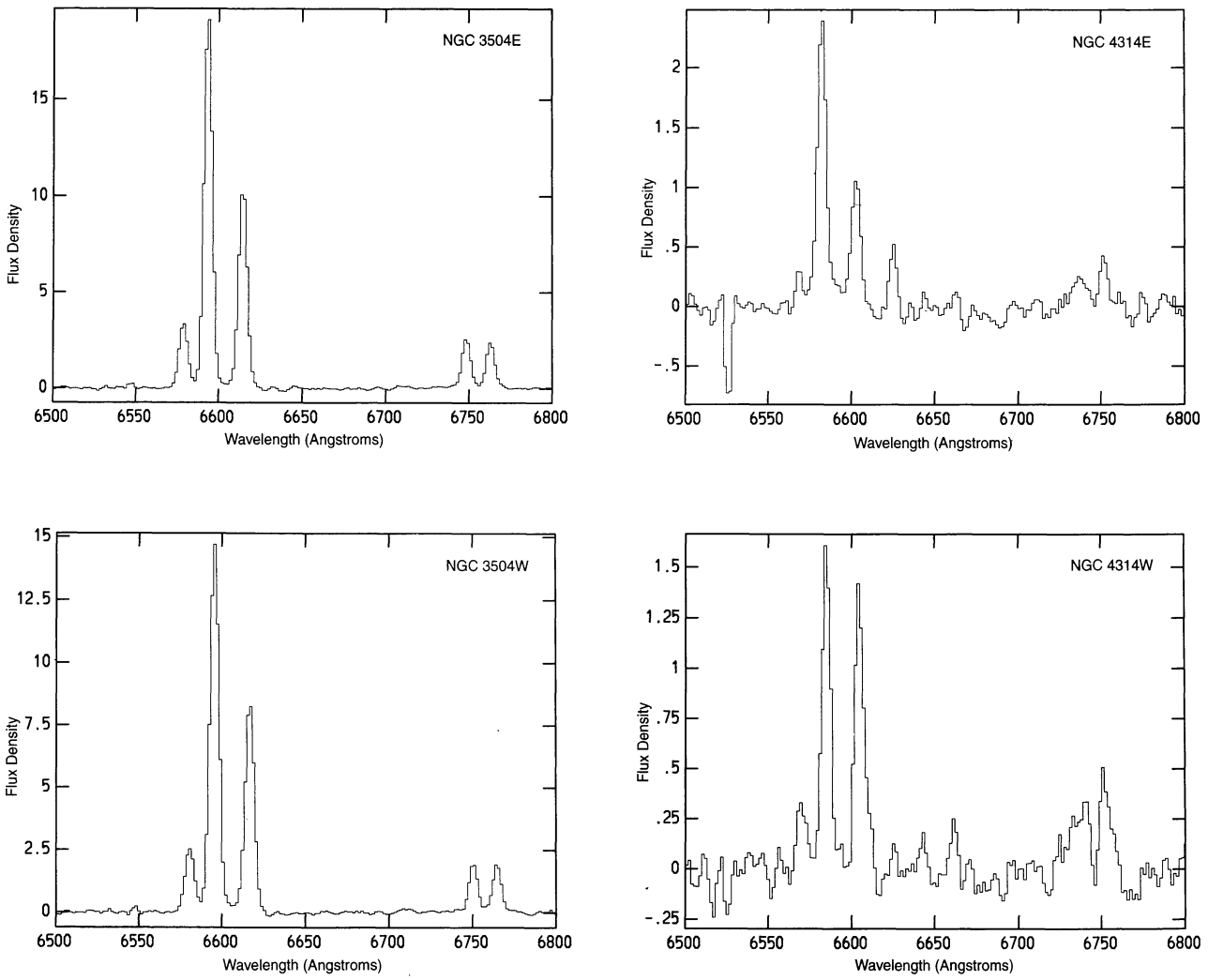

Fig. 2. Spectra from the eastern (upper) and western (lower) circumnuclear regions of bright barred spiral galaxies calibrated in wavelength, sky, flux, and redshift. The position of the slit was always at the PA 90°. Flux units are 10^{-15} ergs s^{-1} cm^{-2} $Å^{-1}$.

have been produced. Figure 2 shows the spectra of the eight galaxies from their eastern and western circumnuclear regions. Ten galaxies did not show any bright emission away from their central pixels and a final spectrum for each of them was obtained after adding the central 5 to 20 pixels.

The task "splot" was used to measure the strengths, central wavelengths, widths, and fluxes of the emission lines. The central wavelengths, widths and fluxes of emission lines were estimated by fitting gaussian curves with the IRAF task splot. For this purpose we fitted multiple curves in order to account for blended broad lines and when possible corroborated the values by fitting individual lines. The velocities were determined with the relation $v = c \times (\lambda_{obs} - \lambda_{rest})/\lambda_{rest}$. The velocities listed in Tables 2 and 3 are heliocentric velocities. The uncertainty for the velocity centroids of the emission lines amounts to about 25 km s^{-1} as a result of wavelength calibration and gaussian fitting. The instrumental spectral resolution was estimated by calculating the full width at half maximum of emission lines of a lamp at different wavelengths across the band. Our estimated value is $FWHM_{inst} \sim 3.23 \pm 0.1$ Å or about 145 ± 5 km s^{-1}. The tabulated line widths were corrected for instrumental resolution by subtracting the instrumental width in quadratures from the observed width: $FWHM^2_{real} = FWHM^2_{obs} - FWHM^2_{inst}$.

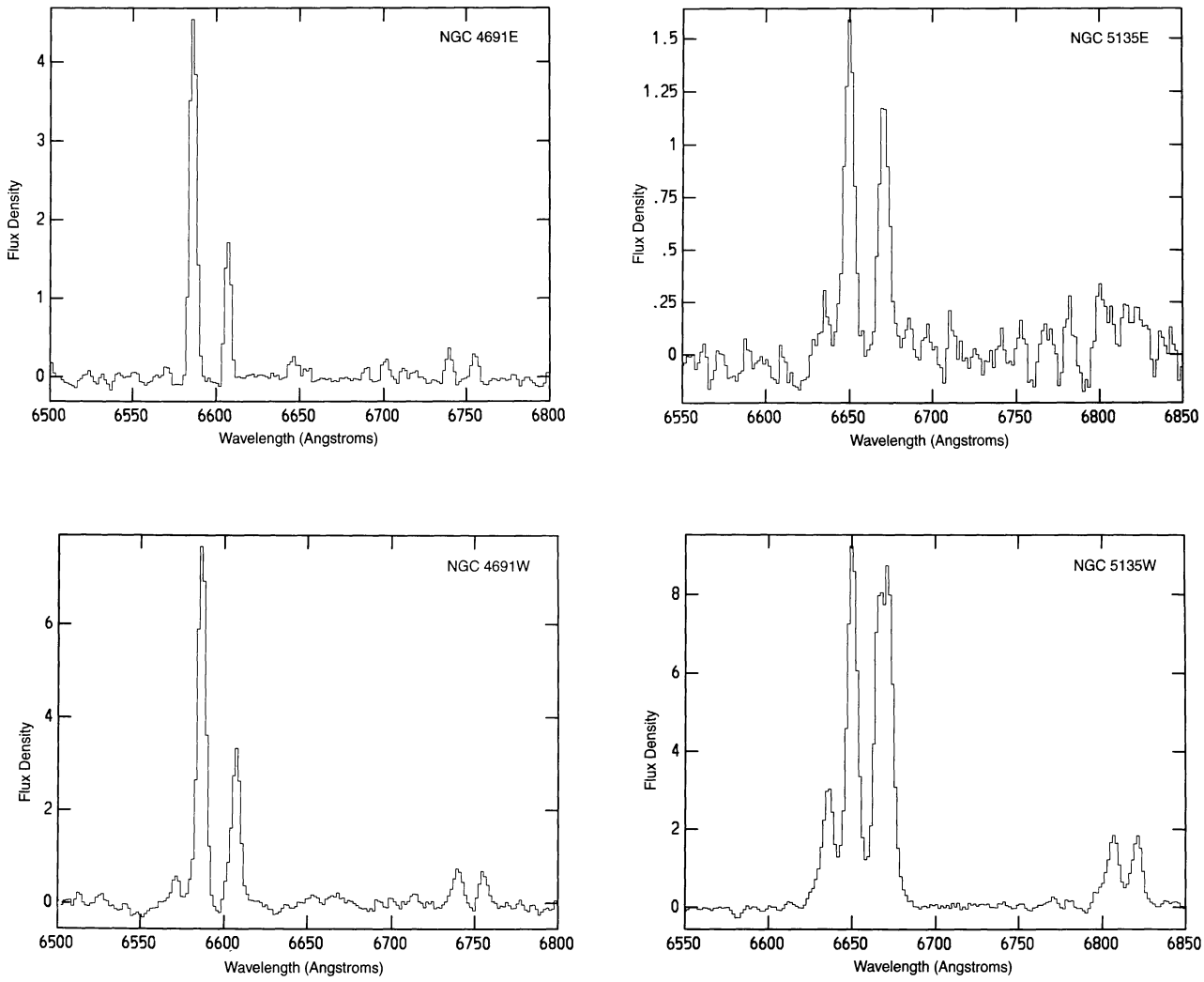

Fig. 2. (Continued)

3. RESULTS AND DISCUSSION

In this section, we present the results of our observations: first, we provide the estimates of central masses calculated from the observed velocities, assuming that the ionized gas rotates on circular orbits around the compact nucleus and lies on the plane of each galaxy's disk. The velocities may also be useful in deriving the properties of resonances using density wave theory and theory of orbits in order to associate circumnuclear structures with Inner Lindblad Resonances (see Binney & Tremaine 1987; Contopoulos & Grosbøl 1989). The spatial distribution of Hα+[N II] of these barred galaxies, except for NGC 5383, has been reported by Pogge (1989a,b) and García-Barreto (1996). Then, the line ratios and electron densities can be derived.

3.1. *Velocities and Inner Masses*

Table 2 lists the heliocentric velocities from the eastern and western sides, in km s^{-1}, for [N II] λ6548.1, Hα λ6562.8, [N II] λ6583.4 and [S II] λ6716.4, and λ6730.8 lines from the 8 galaxies we where were able to isolate the emission. Table 3 lists the heliocentric velocities for other 10 galaxies with no emission away from the central pixels in our slit.

Since the velocities listed in Table 2 are determined from regions off nucleus, they indicate velocities of gas rotating around the center under the influence of the gravitational potential of a galaxy and should not indicate the systemic velocity. Our observations, however, can help us to understand the discrepancy in the different values published for

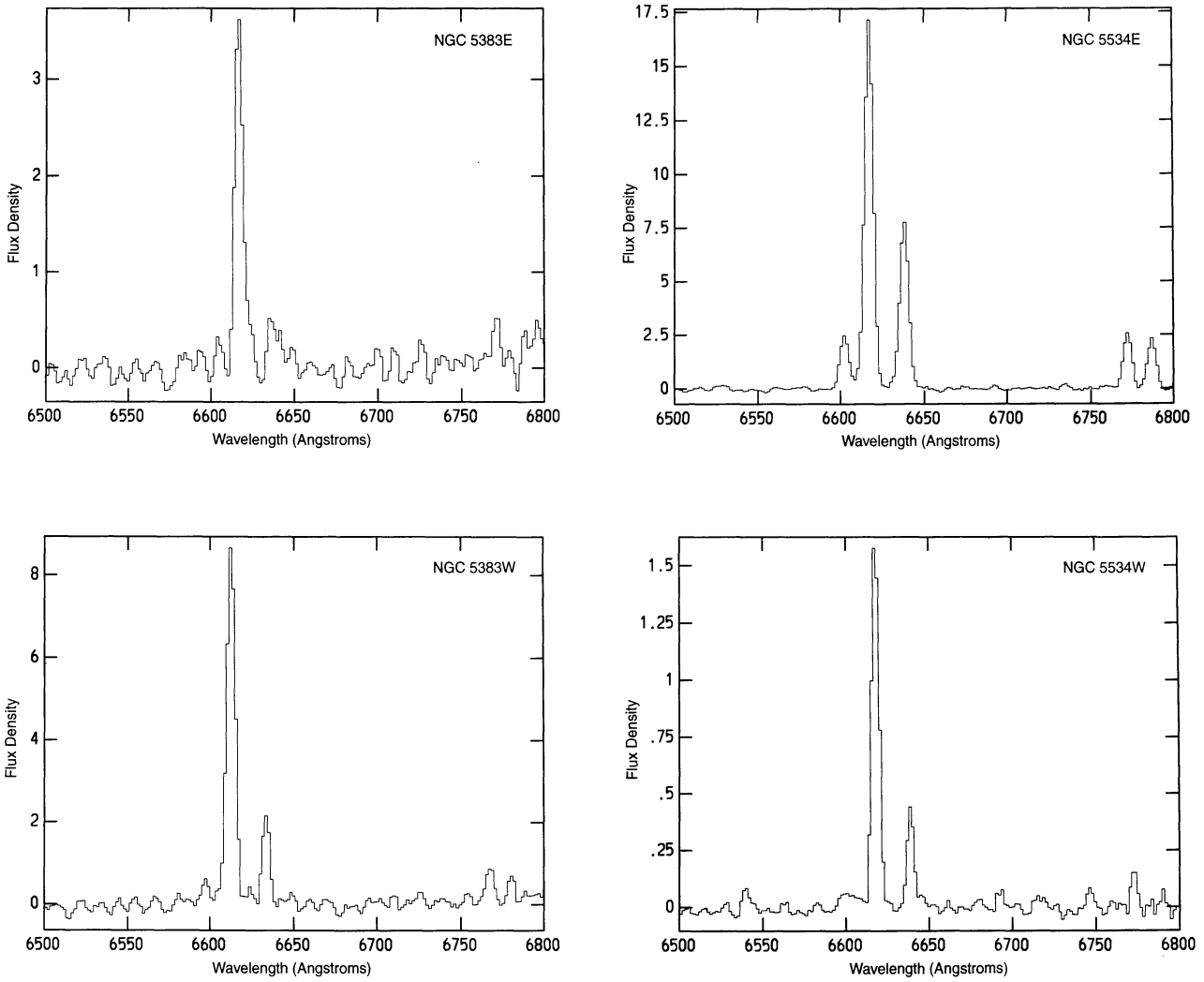

Fig. 2. (Continued)

systemic velocities of barred galaxies; for example, our observations indicate that the different systemic velocities reported in the literature for NGC 4314 (v_{sys} = 883 km s^{-1} [Sandage & Tammann 1987]; v_{sys} = 1004 kms^{-1} [Smith et al. 1987; Strauss et al. 1992]) are most likely the result of their position of the slit relative to the circumnuclear structure. These velocities agree with our observed velocities for the eastern and western regions of a circumnuclear structure (see Table 2). Our optical velocities are somewhat smaller than the velocities obtained from CO lines. In particular, the eastern CO emission peaks at around $v_{east} \approx 920$ km s^{-1} and the western CO emission peaks at around $v_{west} \approx 1030$ km s^{-1} (Benedict, Smith, & Kenney 1996). The differences between optical and CO lines may be the result of hydrodynamic processes at play, e.g., molecular outflows, supernovae events, etc., that may produce a different velocity for the molecular and atomic components.

In NGC 5430, we only detected a velocity of $v \approx 3065$ km s^{-1}, which is quite different from the reported systemic optical velocity of v_{sys} = 2875 km s^{-1}. On the other hand, the CO lines have $v_{NE} \approx 2893$ km s^{-1} and $v_{SW} \approx 3069$ km s^{-1} (Contini et al. 1997). This leads us to conclude that our spectrum only showed the emission from the south-western (SW) blob, and that the reported systemic velocity is probably better associated to the NE blob.

Our velocities for NGC 4691 and NGC 6951 are in agreement with the velocities reported by Wiklind, Henkel, & Sage (1993) and by Boer & Schulz

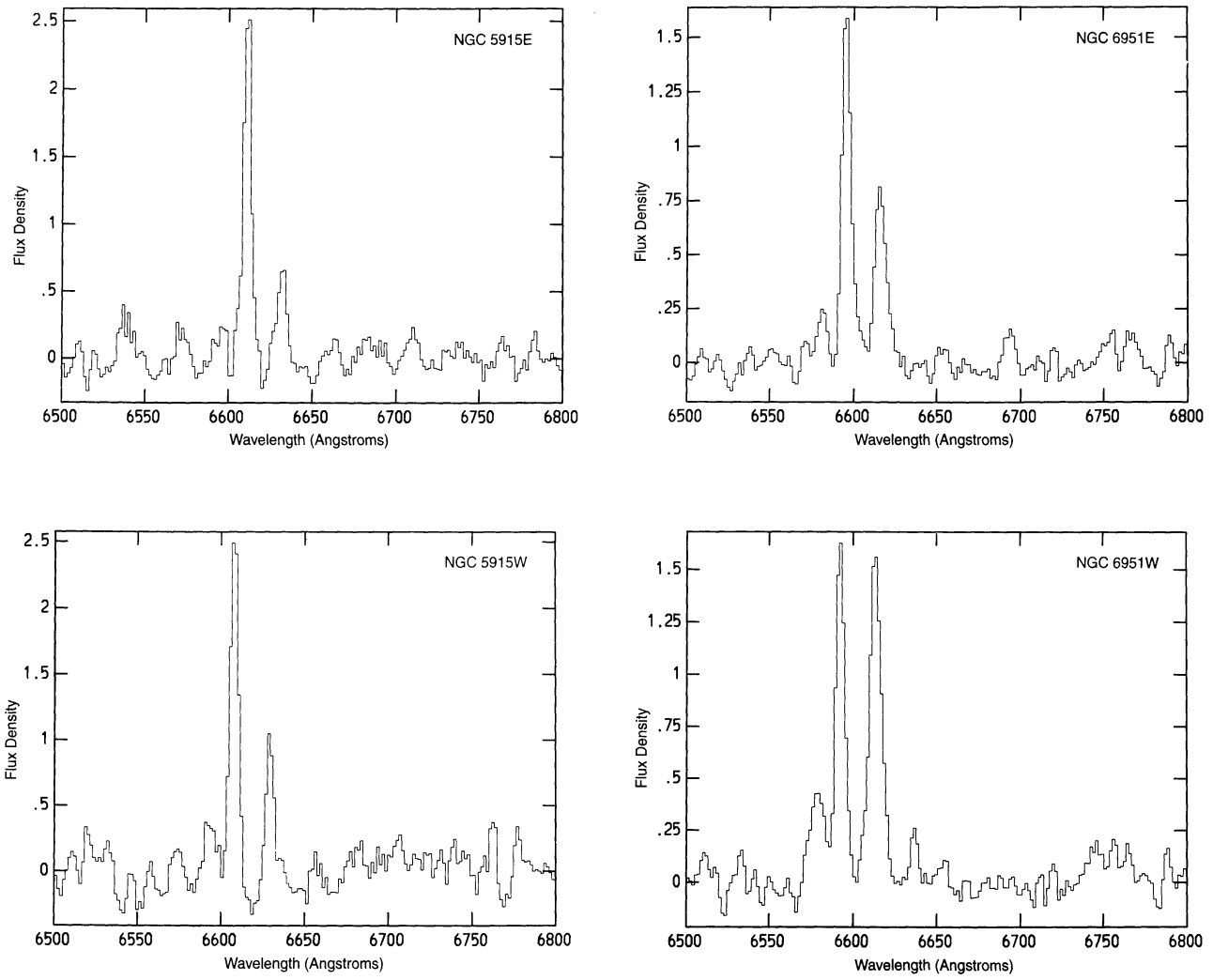

Fig. 2. (Continued)

(1993). The optical velocities for NGC 3504 differ by $\approx$ 100 km s^{-1} from the CO velocities. This discrepancy is likely the result of positioning the slit off the nucleus (e.g., Kenney et al. 1992). Table 4 lists the velocity differences for the galaxies observed.

We estimate the dynamical mass interior to the rings of ionized matter. Assuming that most of the mass interior to these rings is homogeneously distributed inside a radius R, the dynamical mass may be estimated from $(M_{dyn}/M_{\odot}) = 233.7\ (R/\mathrm{pc})\ (V_{true}/\mathrm{km\ s^{-1}})^2$, where $V_{true} = V_{obs}/\sin(i)$, with V_{obs} the observed velocity, and i is the inclination angle of the circumnuclear structure with respect to the plane of the sky. We are assuming, not necessarily being correct, that the circumnuclear structure is on the plane of a given galaxy and its inclination is the same as the inclination of the galaxy disk. This assumption is based primarily on the idea that circumnuclear structures are at distances of about 300 pc up to 1 kpc from the compact nucleus and such a large structure would be unstable if being inclined with respect to the plane of the disk. In addition, we are implicitly assuming circular orbits for the gas in the rings, which might not be true especially in the presence of a pronounced bar.

Table 5 gives the estimated dynamical masses, M_{dyn}, assuming as we said before that the ionized gas in circumnuclear regions lies in the plane of the Galaxy's disk, and that they follow circular orbits as a response to a central axisymmetric gravitational potential. As mentioned earlier, if circumnuclear structures (i.e., rings) are to be explained as Inner

TABLE 3

EMISSION LINES FROM GALAXIES WITH ONLY A CENTRAL SPECTRUM

Gal.	Reg.	Pix[a]	[N II][b]	[N II]/Hα	Hα[b]	FWHM[c]	Hα Flux[d]	[N II][b]	[N II]/Hα	[S II][b]	[S II]/Hα	[S II][b]	[S II]/Hα
4123	N	12	1211	0.15	1193	251	11.3	1196	0.51	1239	0.14	1215	0.12
4477	N	13	1355	0.70	1373	205	0.8	1375	2.37	1410	0.39	1404	0.57
5347	N	10	2349	0.25	2325	384	2.1	2291	0.71	2349	0.34	2329	0.35
5430	N	10	3073	0.19	3055	320	5.4	3051	0.54	3070	0.14	3101	0.11
5597	N	17	2491	0.15	2452	269	19.0	2467	0.44	2493	0.10	2605	0.06
5691	N	13	...	...	1733	164	0.6	...	...	1745	0.19	1831	0.25
5728	N	14	2852	0.45	2870	507	6.2	2850	1.39	2857	0.40	2865	0.32
5757	N	5	2517	0.14	2505	283	15.9	2516	0.45	2530	0.11	2533	0.11
6239	N	20	...	...	1060	132	4.8	1061	0.12	1061	0.10	1072	0.05
6907	N	18	2968	0.16	2940	347	9.2	2947	0.45	2925	0.09	3002	0.07

[a] Pixels added in slit for central region to produce the final spectrum.
[b] Observed heliocentric velocity centroids in km s^{-1}. The velocity centroid uncertainties amount to about 25 km s^{-1} as a result of wavelength calibration and gaussian fitting. Columns 4 and 5 correspond [N II] λ6548.1 Å; columns 9 and 10 to [N II] λ6583.4 Å; columns 11 and 12 to [S II] λ6716.4 Å, and columns 13 and 14 to [S II] λ6730.8 Å.
[c] Hα full width at half maximum, in km s^{-1}, after deconvolution with an instrumental response ($FWHM_{inst}$∼3.23 ± 0.1 Å = 145 ± 5 km s^{-1}).
[d] Hα flux in units of 10^{-14} ergs s^{-1} cm^{-2}.

TABLE 4

EAST-WEST VELOCITY DIFFERENCES AND LINE RATIOS

Galaxy	ΔV^{a}_{e-n}	ΔV^{a}_{e-w}	ΔV_{n-w}[a]	[S II]/[S II][b]	n_e (cm^{-3})[c]
3504	−39	−87	−48	1.0	∼ 1000 ± 600
4314	...	−115	...	0.6	∼ 4500 ±1000
4691	−18	− 5	13	1.1	∼ 750 ± 250
5135	− 1	−23	−22	1.1	∼ 750 ± 250
5383	...	196	...	1.2	∼ 500 ± 200
5534	...	−25	...	1.0	∼ 1000 ± 600
5915	74	146	72	1.0	∼ 1000 ± 600
6951	63	143	80	0.9	∼ 1600 ± 600

[a] Hα velocity differences in km^{-1}: *e-n* means east minus nucleus; *e-w* means east minus west, and *n-w* means nucleus minus west. All velocities are taken from Tables 2, 3, and 4.
[b] Average (east, west) sulfur line ratio [S II] λ6716.4 Å over [S II] λ6730.8 Å.
[c] Approximate electron densities (Osterbrock 1989).

Lindblad Resonances, more observations are needed in order to have the complete radial velocity field (rotation curves) and to compute epicyclic frequencies, $\kappa(r)$. We estimate an error of about a factor of two on the masses presented in Table 5.

3.2. *Line Ratios and Electron Densities*

3.2.1. [N II]/Hα Ratio

Burbidge & Burbidge (1962) showed that the regions in external galaxies with Hα and [N II] emission

TABLE 5

ESTIMATES OF DYNAMICAL CENTRAL MASSES

Galaxy	Distance[a]	R(pc)	$V = V_{obs}/\sin(i)$[b]	M_{dyn}[c]
3504	26.5	560	83	8.5×10^8
4314	10.0	390	115	1×10^9
4691	22.5	480	34	1.3×10^8
5135	53.2	755	24	1×10^8
5383	37.8	1740	150	9×10^9
5534	35.0	1730	25	2.4×10^8
5915	33.7	1430	108	4×10^9
6951	24.1	595	170	4×10^9

[a] In Mpc from Tully (1988).

[b] True velocity difference, in km s^{-1}, between the nucleus and the west (east) side in NGC 3504, (NGC 4691), NGC 5135, NGC 5383, NGC 5915, and NGC 6951. True velocity half difference between the east and west sides in NGC 4314 and in NGC 5534, for which we assumed an inclination of 30°.

[c] Dynamical mass of each galaxy inside a radius R, in units of solar masses: $(M_{dyn}/M_\odot) = 233.7\ (R/\mathrm{pc})^2\ (V/\mathrm{km\ s^{-1}})^2$.

lines, and a line intensity ratio of [N II] λ6583/Hα $\sim$ 0.33, have a degree of excitation that is similar to the extended H II regions in our own Galaxy. They also pointed out that the observed ratio is larger than 1 in the nucleus of some galaxies. More recent observations of several emission lines, with better sensitivity and spectral coverage, have been used to determine the excitation mechanisms in different objects (Baldwin, Phillips, & Terlevich 1981; Osterbrock 1989). In particular, the emission lines used are: [Ne V] λ3426, [O II] λ3727, Hβ λ4861, He II λ4686, [O III] λ5007, [O I] λ6300, Hα λ6563, [N II] λ6584. Depending on the line ratios, the excitation mechanisms for the line-emitting gas could be: a) photoionization by OB stars, b) photoionization by a power-law continuum source, c) collisional ionization from shock waves, and d) a combination of the above.

Actually, the nuclear regions are usually excited by a power-law source but the circumnuclear rings are excited by UV radiation from recently formed stars. Recent spectroscopic surveys of spiral galaxies show low-ionization emission, suggesting that a flat-spectrum (power law) radiation field photoionizes the nuclear gas (Keel 1983a,b,c; Kennicutt & Kent 1983; Filippenko & Sargent 1985; Ho et al. 1995, 1997a,b; Ho et al. 1997). In the nucleus of Seyfert galaxies the same mechanism seems to operate and high-ionization emission iron lines are found from the central regions, such as: [Fe VII] λ5721, [Fe VII] λ6087, [Fe X] λ6374, and [Fe XIV] λ5303 (Appenzeller & Östreicher 1988). In contrast, several observations support the idea that circumnuclear rings are regions of massive OB star formation: e.g., those with bright Hα emission, 10μm emission, radio continuum emission, and CO mm line emission (e.g., Hummel, van der Hulst, & Keel 1987; García-Barreto et al. 1991a,b; Kenney et al. 1992; Telesco, Dressel, & Wolstencroft 1993; Vila-Vilaró et al. 1995; Benedict et al. 1996; Contini et al. 1997). This is in line with the expectations from galactic dynamics, where large accumulations of material can occur at regions near Lindblad resonances; hence, providing suitable conditions for triggering the formation of stars. Our results corroborate these views, and we find that the photionizing agents for the nuclear gas and the circumnuclear rings are of different nature.

The line ratios [N II]/Hα and [S II]/Hα were computed separately for the eastern and western regions for all galaxies with circumnuclear structures. The [N II] λ6548/Hα ratio is on average $\sim$ 0.12 in the eastern side, $\sim$ 0.16 in the western side (Table 2). The ratio is $\sim$ 0.25 for galaxies without extranuclear emission (Table 3). The [N II] λ6583/Hα ratio is on the average $\sim$ 0.43 in the eastern side and $\sim$ 0.58 in the western side. The average ratio is $\sim$ 0.78 for galaxies presenting spectra from their central regions without circumnuclear structures. The values found are in agreement with the values found in other barred galaxies like NGC 1097 (Phillips et al. 1984).

In the case of NGC 4314 and NGC 6951, with clear circumnuclear rings, the line ratio was found different from each side of the ring. The [N II] λ6583/Hα ratios in NGC 4314 are 0.45 and 0.85 while in NGC 6951 they are 0.48 and 0.93 from their east-

ern and western circumnuclear regions, respectively. Large [N II] λ6583/Hα ratios may be indicative of excitation, but it could also indicate a difference in metallicity. Although in our Galaxy metallicity increases with deacreasing distance to the Galactic center (Peimbert 1979; Güsten & Mezger 1983; Esteban & Peimbert 1995), barred galaxies tend to have very small gradients (Roy 1996). Circumnuclear rings, on the other hand, are usually associated to bursts of star formation due to density enhancement and star evolution (i.e., SN and SNR) (Franco et al. 1998) may induce shock excitation on the [N II] emission. Thus high [N II]/Hα ratios suggest different intrinsic physical conditions, as a result of local star formation and evolution in each side of the ring, but our observations are not suited to disentagle which one of the mentioned effect is most prominent. We believe that the ratio of [N II] λ6583/Hα of 1.01 quoted by Ho et al. 1997b for NGC 4314, represents the ratio from the western side of the circumnuclear ring and not necessarily from the compact nucleus since images suggest that there is no Hα emission from the compact nucleus (Pogge 1989a; García-Barreto et al. 1996). Additionally, the ratio [N II] λ6583/Hα from the compact nucleus of NGC 6951 is about 2, in agreement with previous values reported (Ho et al. 1997b). Figure 3 shows the spectrum corresponding to the compact nucleus of NGC 6951. NGC 4477 and NGC 5728 also show a ratio of [N II] λ6583/Hα of $\sim$ 2.4 and $\sim$ 1.4 respectively, in accord to values found previously (Phillips et al. 1984; Schommer et al. 1988; Ho et al. 1997b). These galaxies are classified as Seyfert 2 galaxies with physical characteristics that account for the ratio observed in the nucleus (Kennicutt, Keel, & Blaha 1989; Ho et al. 1997a,b).

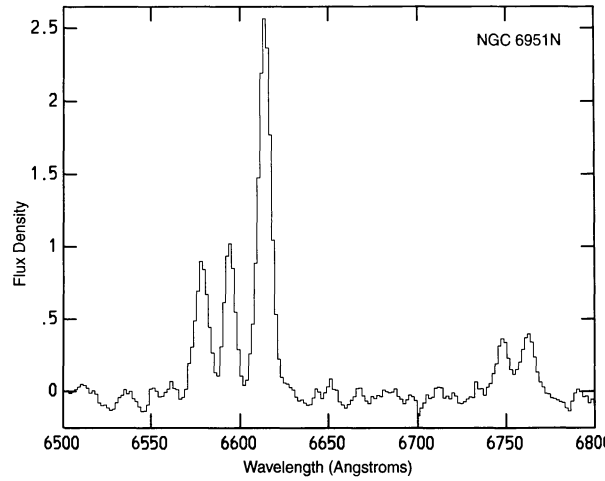

Fig. 3. Spectrum from the compact nucleus in the barred galaxy NGC 6951 calibrated in wavelength, sky, flux, and redshift. Notice that the Hα intensity is much lower than the [N II] λ6583. Flux units are 10^{-15} ergs s^{-1} cm^{-2} Å^{-1}.

3.2.2. [S II]/Hα and [S II] λ6716/[S II] λ6731

The ratio of [S II]/Hα is found in the range from 0.07 to 0.2 with no obvious difference in either side of circumnuclear regions. It is in the range from 0.1 to 0.3 from the compact nucleus in galaxies with circumnuclear structures and it is 0.1 to 0.4 in central regions of galaxies without circumnuclear regions (see Tables 2 and 3). The lower values seem to be from the eastern and western side of the nuclei, but further observations with longer integration times and wider slits are needed to confirm this. Ratios with larger values from nuclei and low values from circumnuclear regions have been found in NGC 1097 (Phillips et al. 1984) and NGC 5728 (Schommer et al. 1988).

The [S II] λ6716/[S II] λ6731 ratio was found to be in the interval from 0.6 to 1.4, suggesting electron densities of a few hundred particles per cm^3 (see Tables 4 and 6; e.g., Osterbrock 1989).

TABLE 6

LINE RATIOS

Galaxy	[S II]/[S II][a]	n_e (cm^{-3})[b]	Galaxy	[S II]/[S II][a]	n_e (cm^{-3})[b]
4123	1.1	$\sim$ 750 $\pm$ 250	5691	0.9	$\sim$ 1600 $\pm$ 600
4477	0.7	$\sim$ 3500 $\pm$ 750	5728	1.2	$\sim$ 500 $\pm$ 200
5347	1.0	$\sim$ 1200 $\pm$ 600	5757	1.0	$\sim$ 1200 $\pm$ 600
5430	1.2	$\sim$ 500 $\pm$ 200	6239	$\sim$ 2.0	$<$ 100
5597	1.5	$\leq$ 100	6907	$\sim$ 1.3	$\sim$ 300 $\pm$ 200

[a] Sulfur line ratio [S II] λ6716.4 Å over [S II] λ6730.8 Å.

[b] Approximate electron densities (Osterbrock 1989).

4. SUMMARY

We have presented new long slit spectroscopic observations with [N II], Hα, and [S II] emission lines from 18 RSA barred spiral galaxies, eight of which have structures around the nucleus. The main results are the following: a) we were able to determine the heliocentric optical velocities for the ionized gas from the compact nucleus, and the eastern and western regions, in eight galaxies. With these velocities we have estimated the inner dynamical mass of each galaxy assuming that the gas move in circular orbits on the plane of the Galaxy. b) We were able to estimate the line ratios [N II] λ6548/Hα, [N II] λ6583/Hα, [S II] λ6716/Hα, and [S II] λ6730/Hα (for the eastern, western, and compact nuclear regions, separately), of eight galaxies. In particular, we found that in galaxies with clear circumnuclear rings, as in NGC 4314 and NGC 6951, the ratio [N II] λ6583/Hα is lower in the eastern region than in the western region of the ring suggesting different local physical conditions as a result of star formation and evolution. c) In NGC 4477, NGC 5728, and NGC 6951 we found that the ratio [N II] λ6583/Hα is larger than unity in the central nuclear regions, in agreement with values reported.

We acknowledge useful comments from the referee that helped us to improve the final version of this paper. J.A.G-B acknowledges partial financial support from DGAPA (UNAM) and CONACyT (971010), México, that allowed him to spend his sabbatical year at the Astronomy Department of the University of Minnesota. He would like to thank the Astronomy Department at UMinn, for their hospitality where part of the original article was written. H.A. thanks the Spanish Ministry of Foreign Affairs for financial support. J.F. acknowledges the support given to this project by DGAPA-UNAM grant, CONACyT grants 400354-5-4843E and 400354-5-0639PE, and a R&D Cray research grant. This research has made use of the NASA/IPAC extragalactic database (NED) which is operated by the Jet Propulsion Laboratory, Caltech, under contract with the National Aeronautics and Space Administration.

REFERENCES

Appenzeller, I., & Östreicher, R. 1988, AJ, 95, 45
Arsenault, R., Boulesteix, J., Georgelin, Y., & Roy, J.-R. 1988, A&A, 200, 29
Baldwin, J. A., Phillips, M. M., & Terlevich, R. 1981, PASP, 93, 5
Barth, A. J., Ho, L. C., Filippenko, A. V., & Sargent, W. L. W. 1995, AJ, 110, 1009
Benedict, G. F., Smith, B. J., & Kenney, J. D. P. 1996, AJ, 111, 1861
Binney, J., & Tremaine, S. 1987, Galactic Dynamics (New Jersey: Princeton, Univ. Press)
Boer, B., & Schulz, H. 1993, A&A, 277, 397
Burbidge, M., & Burbidge, G. R. 1960a, ApJ, 132, 30
_____. 1960b, ApJ, 132, 654
_____. 1962, ApJ, 135, 694
_____. 1964, ApJ, 140, 1445
_____. 1965, ApJ, 142, 634
Burbidge, M., Burbidge, G. R., & Prendergast, K. H. 1960, ApJ, 132, 661
Buta, R. 1986, ApJS, 61, 639
_____. 1995, ApJS, 96, 39
Buta, R., & Crocker, D. D. 1991, AJ, 102, 1715
Contini, T., Wozniak, H., Considere, S. G., & Davoust, E. 1997, A&A, 324, 41
Contopoulos, G., & Grosbøl, P. 1989, A&AR, 1, 261
Esteban, C., & Peimbert, M. 1995, RevMexAASC 3, The Fifth Mexico-Texas Conference on Astrophysics: Gaseous Nebulae and Star Formation, ed. M. Peña & S. Kurtz (México, D. F.: Inst. Astron., UNAM), 133
Filippenko, A. V., & Sargent, W. L. W. 1985, ApJS, 57, 503
Franco, J., Diaz-Miller, R. I., Freyer, T., & García-Segura, G. 1998, in ASP Conf. Ser. Vol. 141, Astrophysics from Antartica, ed. G. Novak & R. H. Landsberg (San Francisco: ASP), 154
Friedli, D., & Benz, W. 1993, A&A, 268, 65
García-Barreto, J. A., Carrillo, R., Klein, U., & Dahlem, M. 1993, RevMexAA, 25, 31
García-Barreto, J. A., Dettmar, R.-J., Combes, F., Gerin, M., & Koribalski, B. 1991a, RevMexAA, 22, 197
García-Barreto, J. A., Downes, D., Combes, F., Gerin, M., Magri, C., Carrasco, L., & Cruz-González, I. 1991b, A&A, 244, 257
García-Barreto, J. A., Downes, D., & Huchtmeier, W. K. 1994, A&A, 288, 705
García-Barreto, J. A., Franco, J., Guichard, J., & Carrillo, R. 1995, ApJ, 451, 156
García-Barreto, J. A., Franco, J., Carrillo, R., Venegas, S., & Escalante-Ramírez, B. 1996, RevMexAA, 32, 89
Genzel, R., Weitzel, L., Tacconi-Garman, L. E., Blietz, M., Cameron, M., Krabbe, A., Lutz, D. & Sternberg, A. 1995, ApJ, 444, 129
Güsten, R., & Mezger, P. 1983, Vistas Astr., 26, 159
Hamuy, M., Walter, A. R., Suntzeff, N. B., Gigoux, P., Heathcote, S. R., & Phillips, M. M. 1992, PASP, 104, 533
Heckman, T. M., Balick, B., & Crane, P. C. 1980, A&AS, 40, 295
Helou, G. 1986, ApJ, 311, L33
Ho, L. C., Filippenko, A. V., & Sargent, W. L. W. 1995, ApJS, 98, 477
_____. 1997a, ApJ, 487, 591
_____. 1997b, ApJS, 112, 315
Ho, L. C., Filippenko, A. V., Sargent, W .L. W., & Peng, C. Y. 1997, ApJS, 112, 391
Huchtmeier, W. K., & Richter, O-G. 1989, A General Catalog of HI Observations of Galaxies (New York: Springer Verlag)
Hummel, E., van der Hulst, J. M., & Keel, W. C. 1987, A&A, 172, 32
Keel, W. C., 1983a, ApJ, 268, 632
_____. 1983b, ApJ, 269, 466

_____. 1983c, ApJS, 52, 229
Kennicutt, R. C. 1992a, ApJ, 388, 310
_____. 1992b, ApJS, 79, 255
Kennicutt, R. C., Keel, W. C., & Blaha, C. A. 1989, AJ, 97, 1022
Kennicutt, R. C., & Kent, S. M. 1983, AJ, 88, 1094
Kenney, J. D. P., Wilson, C. D., Scoville, N. Z., Devereux, N., & Young, J. S. 1992, ApJ, 395, L79
Massey, P., Strobel, K., Barnes, J. V., & Anderson, E. 1988, ApJ, 395, L78
Noguchi, M. 1988, A&A, 203, 259
Osterbrock, D. E. 1989, Astrophysics of Gaseous Nebulae and Active Galactic Nuclei (Mill Valley California: Univ. Science Books)
Peimbert, M. 1979, in IAU Symp. 84, The Large-Scale Characteristics of the Galaxy, ed. W. B. Burton (Dordrecht: Reidel), 307
Phillips, M. M., Pagel, B. E. J., Edmunds, M. G., & Diaz, A. 1984, MNRAS, 210, 701
Pogge, R. W. 1989a, ApJS, 71, 433
_____. 1989b, ApJ, 345, 730
Roy, J.-R. 1996, in ASP Conf. Ser. Vol. 91, Barred Galaxies, ed. R. Buta, D. A. Crocker, & B. G. Elmegreen (San Francisco: ASP), 63
Sandage, A., & Tammann, G. A. 1987, A Revised Shapley-Ames Catalog of Bright Galaxies (Washington, D.C: Carnegie Institution of Washington)
Schommer, R. A., Caldwell, N., Wilson, A. S., & Baldwin, J. A. 1988, ApJ, 324, 154
Smith, B. J., Kleinmann, S. G., Huchra, J. P,. & Low, F. J. 1987, ApJ, 318, 161
Stauffer, J. R. 1982a, ApJ, 262, 66
_____. 1982b, ApJS, 50, 517
Strauss, M. A., Huchra, J. R., Davis, M., Yahil, A., Fisher, K. B., & Tonry, J. 1992, ApJS, 83, 29
Telesco, C. M., Dressel, L. L., & Wolstencroft, R. D. 1993, ApJ, 414, 120
Tully, R. B. 1988, Nearby Galaxy Catalog (Cambridge: Cambridge Univ. Press)
Vaceli, M. S., Viegas, S. M., Grüenwald, R., & de Souza, R. E. 1997, AJ, 114, 1345
Vila-Vilaró, B., Robinson, A., Pérez, E., Axon, D. J., Baum, S. A., González-Delgado, R. M., Pedlar, A., Pérez-Fournon, I., Perry, J. J., & Tadhunter, C. N. 1995, A&A, 302, 58
Wiklind, T., Henkel, C., & Sage, L. J. 1993, A&A, 271, 71
Young, J. S., et al. 1995, ApJS, 98, 219

Héctor Aceves: Instituto de Astrofísica de Andalucía: Apartado Postal 3004, Granada 18080, Spain (aceves@iaa.es).
Gabriela Canalizo: Institute for Astronomy, University of Hawaii, 2680 Woodlawn Drive, Honolulu, HI 96822, U.S.A. (canaguby@galileo.ifa.hawaii.edu).
René Carrillo, J. Antonio García-Barreto, and José Franco: Instituto de Astronomía, UNAM, Apartado Postal 70-264, 04510 México, D.F., México (pepe,rene,tony@astroscu.unam.mx).
Olga Kuhn: Instituto de Astronomía, Observatorio Astronómico Nacional, UNAM, Apartado Postal 877, 22830 Ensenada, B. C., México (olga@bufadora.astrosen.unam.mx).